

Voltammetric Determination of Antidiabetic Drug Gliclazide in the Presence of Glibenclamide in Real Samples

Sayed Zia Mohammadi¹, Somayeh Tajik^{*2,3}, Hamed Tashakkorian^{4,5}, Kaiqiang Zhang⁶, Quyét Van Le^{7,*}, Soma Saeidi⁸, Ho Won Jang⁹, Mohammadreza Shokouhimehr^{9,*} and Wanxi Peng^{10,11,*}

¹ Department of Chemistry, Payame Noor University, Tehran, Iran

² Bam University of Medical Sciences, Bam, Iran

³ Research Center for Tropical and Infectious Diseases, Kerman University of Medical Sciences, Kerman, Iran

⁴ Cellular and Molecular Biology Research Center (CMBRC), Health Research Institute, Babol University of Medical Sciences

⁵ Department of Pharmacology, School of Medicine, Babol University of Medical Sciences, Babol, Iran

⁶ Jiangsu Key Laboratory of Advanced Organic Materials, Key Laboratory of Mesoscopic Chemistry of MOE, School of Chemistry and Chemical Engineering, Nanjing University, Nanjing, Jiangsu 210023, China

⁷ Institute of Research and Development, Duy Tan University, Da Nang 550000, Vietnam

⁸ Department of Molecular Medicine and Biopharmaceutical Sciences, Graduate School of Convergence Science and Technology, Seoul National University, Seoul, South Korea.

⁹ Department of Materials Science and Engineering, Research Institute of Advanced Materials, Seoul National University, Seoul 08826, Republic of Korea

¹⁰ College of Forestry, Henan Agricultural University, Zhengzhou 450002, China

¹¹ School of Automotive Engineering, HuangheJiaotong University, Jiaozuo 454950, China

*E-mail: h.beitollahi@yahoo.com, Levanquyet@dtu.edu.vn, mrsh2@snu.ac.kr, pengwanxi@163.com

Received: 17 May 2020 / Accepted: 7 July 2020 / Published: 10 August 2020

The work describe a modified screen printed electrode (SPE) for the concurrent analysis of gliclazide and glibenclamide. The modification of the SPE was performed using Fe₃O₄nanoparticles (Fe₃O₄NPs) derivative. When used for the oxidation of gliclazide under optimal conditions, the over-potential associated with the oxidation of gliclazide dropped for about 130 mV as opposed to the case of unmodified SPEs. The modified electrodes were used to monitor the electrochemical-behavior of gliclazide through differential pulse voltammetry (DPV) and cyclic voltammetry (CV), and also obtain some kinetic data on gliclazide. The response of the electrode was found to be linear from 0.5 to 600.0 μM and a detection limit of 0.1 μM (based on 3s/m) was reached through DPV. The Fe₃O₄ NP/SPE was applied to the determine gliclazide and glibenclamide in the drug and urine samples. The results indicated satisfactory recovery of two analytes. Hence, it was concluded that the electrode is applicable for the analysis of gliclazide and glibenclamide in drug administration and clinical laboratories.

Keywords: Gliclazide, Glibenclamide, Fe₃O₄ NPs derivative, screen printed electrode, Voltammetry

1. INTRODUCTION

Gliclazide is a sulphonylurea administered for the treatment of type II diabetes, with a similar efficacy to other sulphonylureas, but it has lower risks of hypoglycaemia and cardiovascular side effects. This can be attributed to its selective inhibition activity towards the ATP-sensitive potassium (KATP) channels in pancreas, as well as its relatively lower half-life [1]. Gliclazide is also known to possess excellent antioxidant properties and desirable haemobiological effects [2].

Various analytical approaches have been used for the determination of gliclazide such as chromatography, spectrophotometry and electrophoresis [3-8]. The number of reports on the application of electrochemical methods for the analysis and study of gliclazide are however rather limited [9-11].

Many type II diabetes patients cannot be effectively treated through the administration of one oral antidiabetic agent, in terms of reaching target glycaemic goals [12]. Hence, more than one drug should be used to obtain satisfactory results. Under such circumstances, a combination of different sulphonylureas, *e.g.* gliclazide and glibenclamide (scheme 1) may be administered [13]. Naturally, the determination of concentrations of such antidiabetics is of great importance for pharmacokinetic studies as well as for more typical applications such as monitoring the levels of the drug or the diagnosis of factitious hypoglycaemia [14].

More recent method used for monitoring different drugs include spectroscopic and electrochemical methods [15-28], where the latter offer enhanced selectivity, sensitivity, speed and repeatability, and also require lower costs and time [29-50].

As a promising class of electrochemical tools, SPEs offer advantages of disposability, cost-effective, high reproducibility, high sensitivity, linear and quick response, low power consumption, the possibility of ease modification, and ease of their miniaturization [51-62].

In recent years, the modification of the working electrode surface, to increase the sensitivity and selectivity of electrochemical sensors is considered an essential step [63-74]. In this regard, the modified electrodes have been widely used for sensitive and selective determination of the various targets [75-86].

Recently, Fe₃O₄ NPs have attracted attention due to their unique physical properties, such as, superparamagnetism, high coercivity and low Curie temperature [87-89]. In addition to these characteristics, Fe₃O₄ NPs are non-toxic and biocompatible. Therefore, Fe₃O₄ NPs have brought out some new kinds of biomedical applications such as contrasting agent in magnetic resonance imaging (MRI), dynamic sealing, localizer in therapeutic hyperthermia, biosensors, and magnetic targeted-drug delivery system [90-94].

The present work tends to describe the modification of a SPE using 2-(4-((3-(trimethoxysilyl)propylthio)methyl)-1H-1,2,3-triazol-1-yl)acetic acid-Fe₃O₄NPs (Fe₃O₄ NP derivative), as an analytical tool for the concurrent determination of gliclazide and glibenclamide.

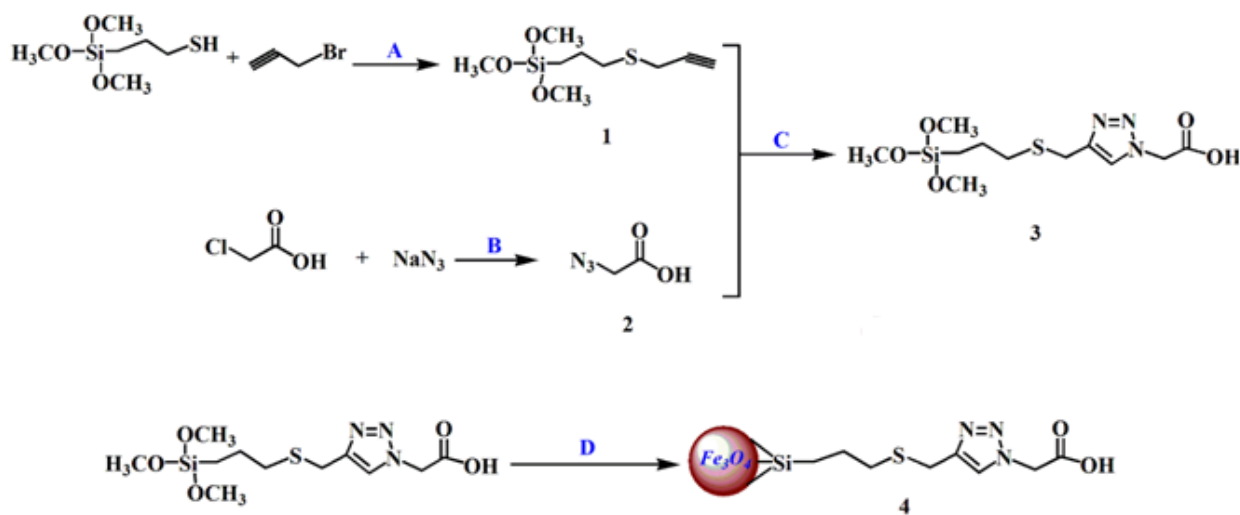
2. EXPERIMENTAL

2.1. Instrumentation and reagents

In this stage, we utilized the Auto-lab potentiostat/galvanostat PGSTAT 302N for electrochemical experimentations. SPE (DropSens; DRP-110; Spain) had 3 conventional electrodes of the graphite as counter electrode, unmodified graphite as working electrode as well as a silver as pseudo-reference electrode. In addition Metrohm 710 pH meter has been used to measure pH. Field emission scanning electron microscopy (FESEM) was recorded on a Hitachi S4160 instrument (Tokyo, Japan). Transmission electron microscopy (TEM) was performed on a CM1 electron microscope at an accelerating voltage of 120 kV (Philips, Netherland). VSM measurements were performed by using a vibrating sample magnetometer (LDJ Electronics Inc., Model 9600). FT-IR spectra were recorded on a Bruker Tensor 27 spectrometer (Bruker, Karlsruhe, Germany).

Gliclazide, glibenclamide as well as all the remaining reagents obtained from Merck. Finally, we utilized the ortho-phosphoric acid and its salts to reach a pH range from 2.0 to 12.0.

2.2. Fabrication of 2-(4-((3-(trimethoxysilyl) propylthio) methyl)-1,2,3-triazol-1-yl) acetic acid- Fe_3O_4 NPs



A: Propargyl Bromide, Potassium Carbonate, Acetone (20 hrs); **B:** Sodium Azide, DMF, 90°C (24 hrs)


C: Copper(II)Sulfate, Sodium Ascorbate, DMF, rt (30 hrs); **D:** Fe_3O_4 NPs;  Toluene, 110 °C

Figure 1. Schematic diagram for preparation of Fe_3O_4 NP derivative.

This modifier was synthesized using the four steps procedure shown schematically in Figure 1 and described as follows:

Step A:

In this step, 0.11 mL of propargyl bromide (1mmole) was poured inside a round-bottomed flask containing 15 ml of acetone with 0.195 mL of 3-mercaptopropyl(trimethoxy) silane (1.05 mmol) and 0.167 g of potassium carbonate (1.2mmole), which were incubated for 20 hours at 70 °C while stirring under N₂, followed by filtering and then evaporating the solvent using rotary evaporator. The result was two-phase extraction (ethylacetate: water) that was washed with NaHCO₃ (5%) and brine solution resulting in oily trimethoxy (3-(prop-2-yn-1-ylthio) propyl) silane that was then incorporated in the next step with no purification. Anal. Calcd for C₉H₁₈O₃SSi: S: 13.67%; H: 7.69%, C: 46.15%, found: S: 13.38%. H:7.25%, C:46.46%;

Step B:

In this step, 0.094 g of chloroacetic acid (1 mmol) solution in DMF (15 mL) was added by 0.072 g of sodium azide (1.05 mmol), followed by stirring for 24 hours at 90 °C and then storing to fabricate the product 3.

Step C:

This compound was synthesized. Reaction between the products prepared from step 1 and step 2 were done on the basis of click protocol which were employed in our previous articles [95, 96] for the preparation of the triazole compounds. Using one-pot production process, the compound 3 was synthesized by augmenting trimethoxy (3-(prop-2-yn-1-ylthio) propyl) silane (1) (1mmol) to fresh DMF (15 ml) solution of 2-azidoacetic acid. Then, 0.075 g of CuSO₄ · 5H₂O (0.3 mmol), 0.346 g of sodium ascorbate (1.5 mmol) and 2 ml of water were mixed with resulting reaction product, stirred for 30 hours at an ambient temperature, and appended to 30 ml of water to exclude the wastes, followed by extraction using 25 ml of ethyl acetate. The product was rinsed by 15 ml of ammonium hydroxide (1N) to delete copper ions unreacted. The washing was repeated for organic phase that was dried over MgSO₄ and filtered. The solvent was excluded by reducing the pressure using rotary evaporator (Heidolph) to extract the oily product 3. Anal. Calcd for C₁₁H₂₁N₃O₅SSi: S: 9.55 H: 6.27%, %;C: 39.40%, N: 12.54%, found: S: 9.28%., H: 5.95%, C: 39.76%; N: 12.34%,

Step D:

The co-precipitation approach was used to prepare the magnetic NPs [97], so that 1.9 g of FeCl₃ · 6H₂O and 0.67 g of FeCl₂ · 4H₂O were added to 50 ml of deionized water to be dissolved under argon atmosphere. After 30 minutes, the solution was added by 3 mL of ammonium hydroxide solution (25%) while maintaining the pH=11 with continuous stirring using a magnetic stirrer. The addition of the whole volume of the ammonia solution immediately resulted in a deep black magnetite precipitate that was stirred for an hour under argon atmosphere. The magnet was used to collect the precipitate that was rinsed by deionized water several times to exclude the additional ammonia to reach pH of neutral eluent water. A dark glass was applied to keep the magnetite NPs for further applications.

One g of magnetic NPs (Fe₃O₄) was appended onto the produced compound 3 solution in DMF (30 ml) inside a 50-ml round-bottomed flask. Maximum dispersion was achieved by sonication the reaction mixture for 10 minutes with the aid of ultrasonic bath and then heating at the temperature of 110 °C for 24 hours under argon atmosphere. Subsequently, the magnet was used to collect Fe₃O₄ NPs

that were respectively rinsed by DMF and acetone, which were then stored in a dark glass inside a desiccator.

2.3. Morphology and structure of Fe_3O_4 NPs derivative

Investigations of the morphology and structure of magnetic NPs were determined by FTIR (fourier-transform infrared spectroscopy), XRD (X-ray diffraction), FESEM (field emission scanning electron microscopy), TEM (transmission electron microscopy) and VSM (vibrating sample magnetometer) techniques and discussed fully in the Results and discussion section.

2.4. Modification of SPEs

Considering a simplified process, Fe_3O_4 NPs derivative has been used to coat the bare SPE. Then, 1 mg Fe_3O_4 NPs derivative has been dispersed in a 1 mL of aqueous solution using ultrasonication duration of 45 min. After that, 1 μ l of the procured suspension has been dropped on working electrode and placed at the room temperature in order to dry it.

3. RESULTS AND DISCUSSION

3.1. Structural characterization

FT-IR spectrum of the product 3 is in Figure 2 compared with that of the product 4 to determine changes that might have taken place upon reaction. The FT-IR spectrum of product 3 C (Fig. 2) exhibits the characteristic bands of the (Si–O–Si), (C–N), (C=N), (C=C), (C=O), (C–CH) and (O–H) which appear at 1122, 1304, 1414, 1628, 1742, 2925 and 3291-3422 (broad peak) cm^{-1} , respectively. In the product 4 (Fig. 2), the stretching vibration for these groups shifts slightly to a lower wave number. Also, the spectrum of the product 4 shows new absorptions in the region of 3300-3500, 1418, and 592 cm^{-1} , attributable to the O–H, Fe–O, and Fe–O–H stretching mode, respectively.

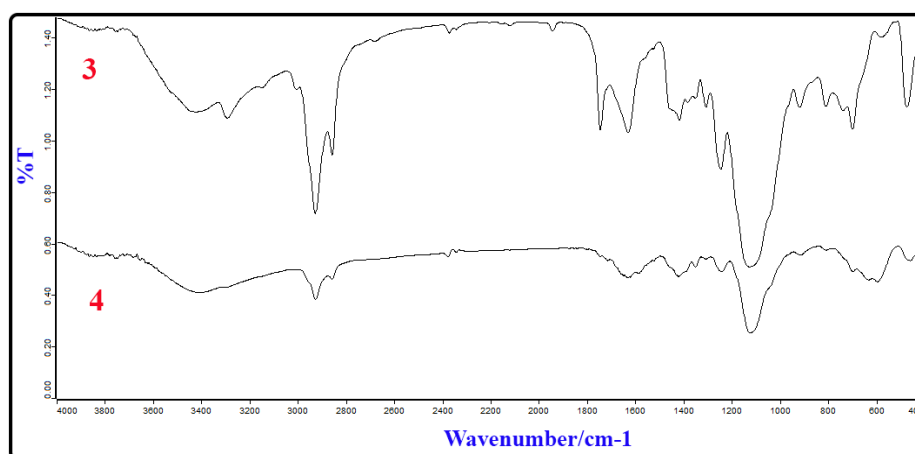


Figure 2. FT-IR spectra of products 3 and 4.

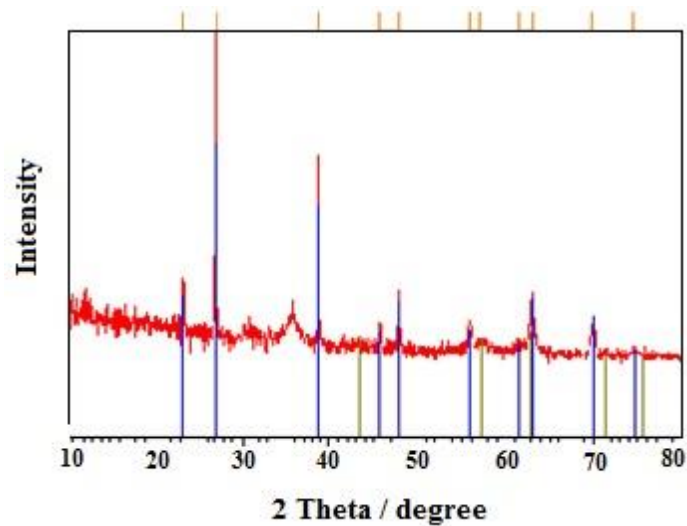


Figure 3.XRD patterns for Fe₃O₄ NP derivative.

Figure 3 presents the XRD patterns of Fe₃O₄ at 2θ in the range of 10–80°. Figure 3 shows a series of diffraction peaks at around 2θ of 30.1°, 35.4°, 43.1°, 53.4°, 57.0° and 62.6° which is related to the reflection of (2 2 0), (3 1 1), (4 0 0), (4 2 2), (5 1 1) and (4 4 0) planes of Fe₃O₄, respectively (JCPDS card No. 19-629) [98]. These peaks are sharp and intense, demonstrating the well crystallized structure of Fe₃O₄ with typical cubic inverse spinel structure.

FESEM and TEM images of magnetic NPs are displayed in Figure 4. The images clearly reveal the shape and dimensions of NPs which are in the range of 30–75 nm.

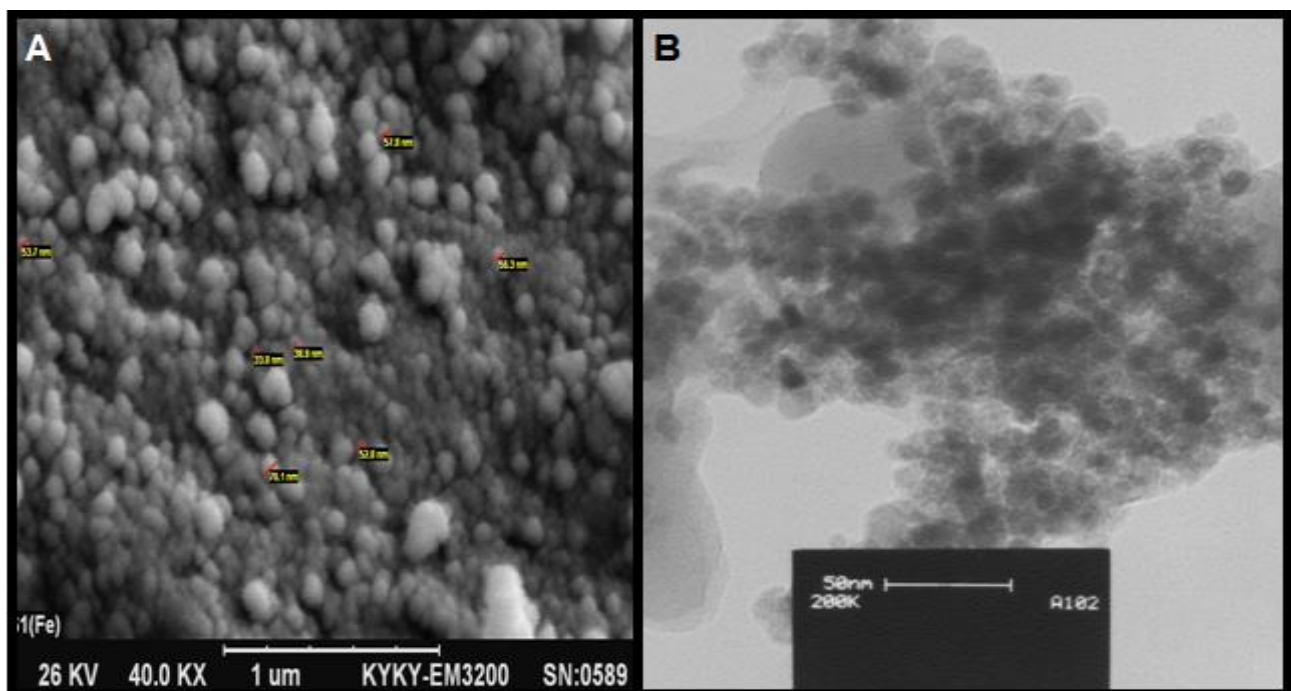


Figure 4. FESEM (A) and TEM (B) images of Fe₃O₄ NP derivative.

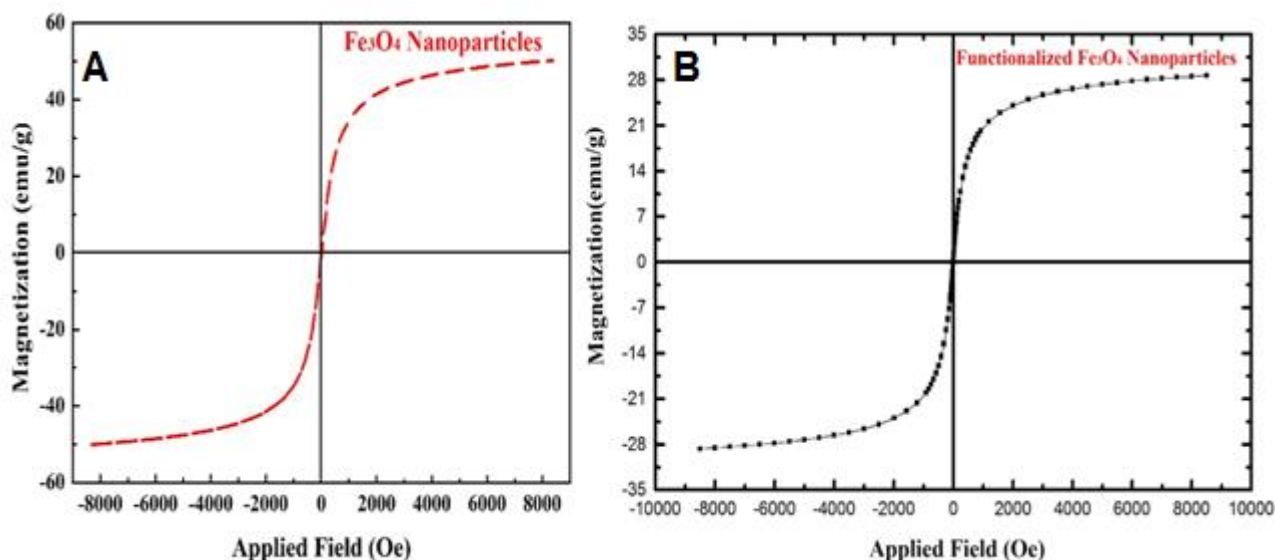


Figure 5. VSM analysis of Fe_3O_4 NP derivative VSM analysis of (A) Bare Fe_3O_4 NPs (B) Functionalized Fe_3O_4 NPs.

In order to assess the effect of the mentioned functionalization on the magnetic properties of Fe_3O_4 NPs derivative, the vibrating sample magnetometer or VSM analysis was applied. Magnetization curves of Fe_3O_4 NPs and Fe_3O_4 NPs derivative are displayed in Figure 5. The result shows that both samples possess super paramagnetic properties at room temperature because of the negligible remanence (M_r) and coercivity (H_c) in the absence of external magnetic field [99]. The result displays that the synthesized magnetic NPs showed a smaller H_c and M_r compared to bare Fe_3O_4 NPs. It can be concluded that the presence of aliphatic groups, triazole rings and carboxylic acid on the surface of Fe_3O_4 can reduce agglomeration of magnetic NPs. Modification of magnetic NPs surface can cause decrease in saturation magnetization value for Fe_3O_4 NPs derivative compared to pure Fe_3O_4 NPs. The saturation magnetization (M_s) of Fe_3O_4 NPs and the prepared functionalized NPs was 50 and 28 emu/g respectively. The result proposed that NPs with acceptable magnetic property beside their active functional groups, can be regarded in variety of applications such as sensing biomolecules, bioassay, removal of hazardous compounds, drug delivery, etc.

3.2. Electrocatalytic oxidation of gliclazide at functionalized Fe_3O_4 NP/SPE

To obtain the optimal results for the electrocatalytic oxidation of gliclazide, the pH of the test solution should be optimized. To determine the optimal pH, gliclazide solutions in PBS with various pHs (2.0 to 9.0) were prepared and analyzed using the modified Fe_3O_4 NP/SPE through cyclic voltammetry technique. The results presented in Figure 6 prove that the electrocatalytic oxidation reaction favors neutral pH, what is indicated by the gradual increase of the anodic peak current. Hence, pH of 7.0 was chosen as the optimal value and used throughout the experiments.

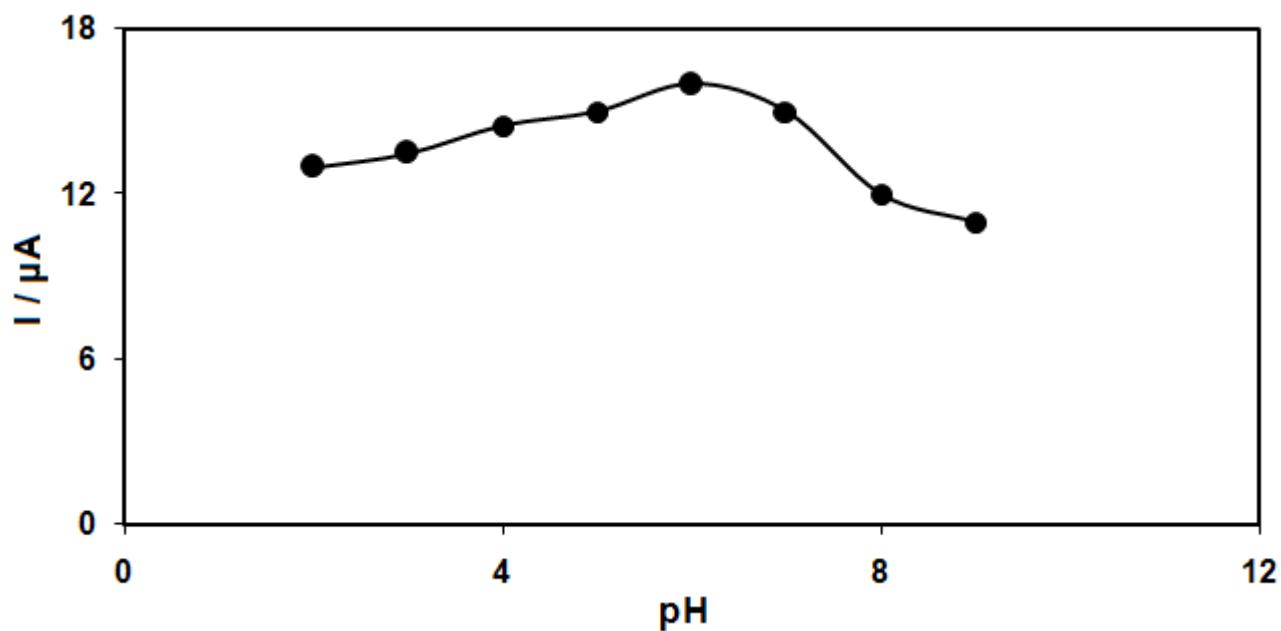


Figure 6. Plot of I_p vs. pH (2.0-9.0) in 200.0 μM gliclazide. Scan rate = 50 mV s^{-1} .

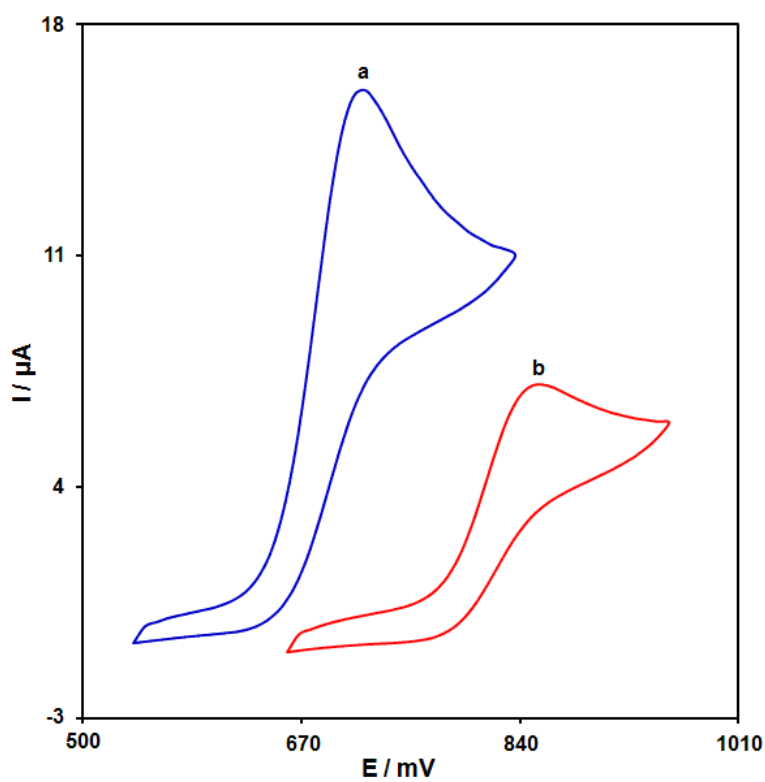


Figure 7. CVs recorded at the scan rate 50 mVs^{-1} in 200.0 μM gliclazide for: (a) Fe_3O_4 NP/SPE and (b) bare SPE.

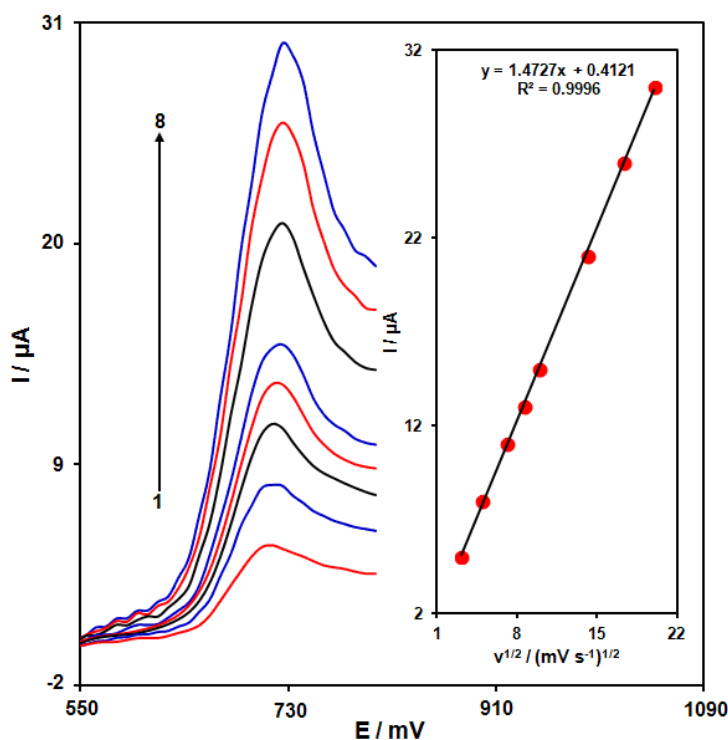


Figure 8. Linear sweep voltammograms (LSVs) of Fe₃O₄ NP/SPE in 100.0 μM gliclazide at various scan rates; (10, 25, 50, 75, 100, 200, 300 and 400 mV s⁻¹). Inset; variations in the anodic peak currents vs. v^{1/2}.

To evaluate the effect of the electrode modification, some tests were performed using the modified electrode and unmodified SPE. The results of cyclic voltammetry of 200.0 μM gliclazide solution presented in Figure 7 and obtained with functionalized Fe₃O₄ NP/SPE (curve a) and unmodified SPE (curve b) clearly reveal that in the case of modified electrode, the maximum oxidation occurs at 720 mV, which is about 140 mV more negative compared to the bare SPE.

The enhanced scan rates resulted in the augmented oxidation peak current (I_p linearly related to the v^{1/2}) (Fig. 8) demonstrating gliclazide oxidation procedure has been diffusion-controlled [100].

3.3. Chronoamperometric studies

The chronoamperometric study was performed by setting the potential of the prepared functionalized Fe₃O₄ NP/SPE at 0.8 V and using different gliclazide concentrations in PBS (pH=7.0) solution, and the results are given in Figure 9.

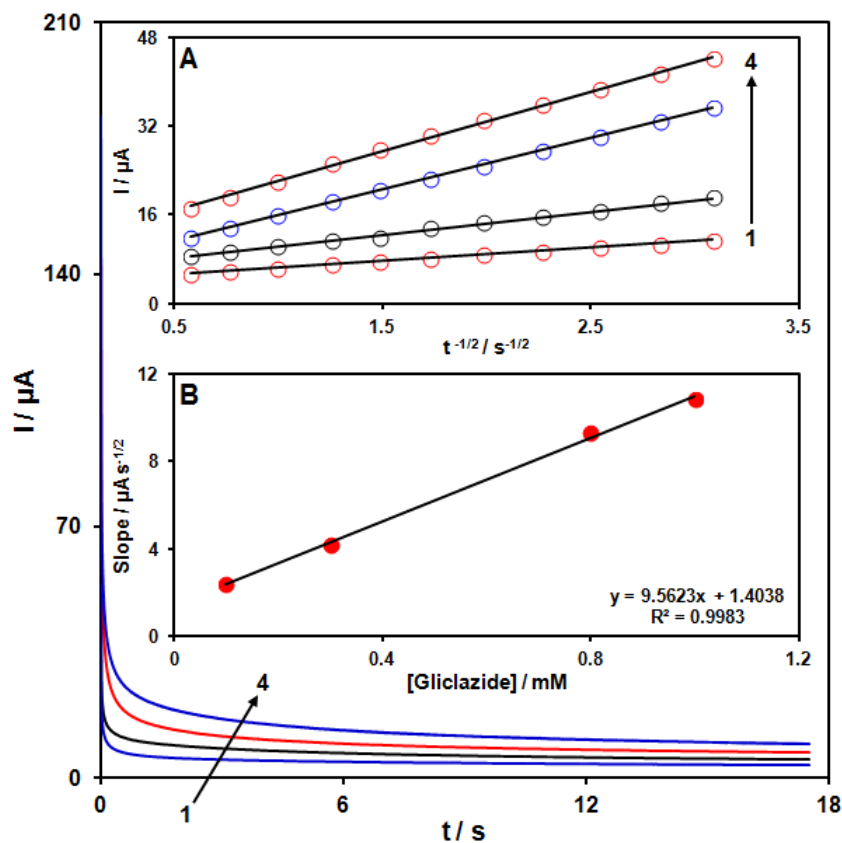


Figure 9. Chronoamperograms obtained at Fe_3O_4 NP/SPE for different concentrations of gliclazide. The numbers 1–4 correspond to 0.1, 0.3, 0.8 and 1.0 mM of gliclazide. Insets: (A) Plots of I vs. $t^{-1/2}$ obtained from chronoamperograms 1–4. (B) Plot of the slope of the straight lines against gliclazide concentration.

Cottrell equation describes the current observed in the electrochemical reaction of an electroactive material with the diffusion coefficient D , under mass transport limited condition [45]. After plotting I vs. $t^{-1/2}$ curves with best fits for various gliclazide concentrations, Figure 9A was obtained. The slopes of plots from Figure 9A plotted against the concentration of gliclazide are presented in Figure 9B. Using the slope from Cottrell equation and Figure 9B, the mean value for D was determined to be $7.8 \times 10^{-6} \text{ cm}^2/\text{s}$.

3.4. Calibration curves and the limits of detection

The peak currents obtained for the electrooxidation of gliclazide at the synthesized Fe_3O_4 NP/SPE can be used to determine the concentration of gliclazide. To obtain the information, DPV experiments were performed on different gliclazide solutions and the resulting peak currents were found proportional to the concentration of gliclazide. According to Figure 10, this trend is observed between 5.0×10^{-7} – 6.0×10^{-4} M and the detection limit (3δ) of the analysis is found to be 1.0×10^{-7} M.

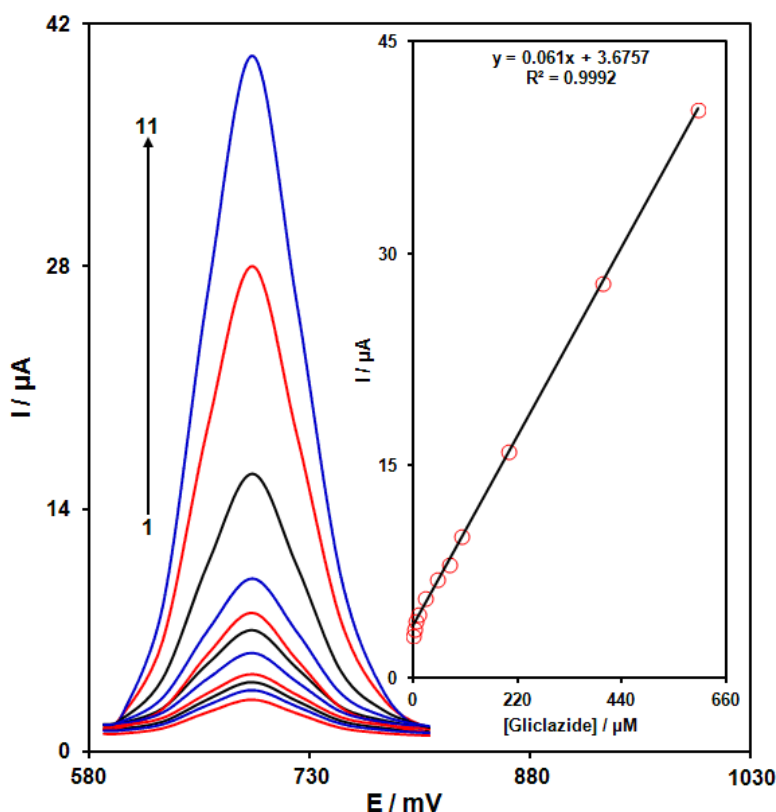


Figure 10. DPVs of Fe₃O₄ NP/SPE for different gliclazide concentrations. Numbers 1–11 correspond to 0.5, 2.0, 5.0, 10.0, 25.0, 50.0, 75.0, 100.0, 200.0, 400.0 and 600.0 μM of gliclazide. Inset: Plot of the I_p as a function of gliclazide concentration in the range of 0.5-600.0 μM.

Table 1. Comparison of the efficiency of some modified electrodes used in the electrocatalysis of gliclazide.

Electrode	Modifier	Limit of Detection	Linear Range	Ref.
Glassy carbon electrode	Electropolymerized molecularly imprinted polypyrrole film	1.2×10 ⁻¹¹	5×10 ⁻¹¹ –4×10 ⁻¹⁰	9
Glassy carbon electrode	β-Cyclodextrin	-	1.0×10 ⁻⁵ – 5.0×10 ⁻⁵	10
Carbon paste electrode	ZnIn ₂ S ₄ NPs (ZIS) and an ionic liquid [1-butyl-3-methylimidazolium hexafluorophosphate, (BMIM.PF ₆)]	1.2 × 10 ⁻⁷	7.5×10 ⁻⁷ –5.0×10 ⁻⁴	11
Glassy carbon electrode	Magnetic core-shell Fe ₃ O ₄ @SiO ₂ and multi-walled carbon nanotubes (MWCNTs)	2.1×10 ⁻⁶	5.0×10 ⁻⁶ –8.0×10 ⁻⁴	66
SPE	Fe ₃ O ₄ NP	1.0 × 10 ⁻⁷	5.0×10 ⁻⁷ –6.0×10 ⁻⁴	This Work

With the glibenclamide samples, the peak currents obtained using the modified Fe₃O₄ NP/SPE are also found to have a linear relationship with the sample concentrations in the range of

2.0×10^{-6} – 7.0×10^{-4} M, and the detection limit (3δ) was determined to be 9.0×10^{-7} M. The results for gliclazide detection are compared with previous works in table 1.

3.5. Concurrent determination of gliclazide and glibenclamide

Glibenclamide causes serious interferences in the electrochemical analysis of gliclazide using bare SPE since the oxidation potentials of the two species are rather close. In this light and knowing that no published reports can be found on the concurrent determination of gliclazide and glibenclamide using the prepared NP/SPE, this concept was put to test.

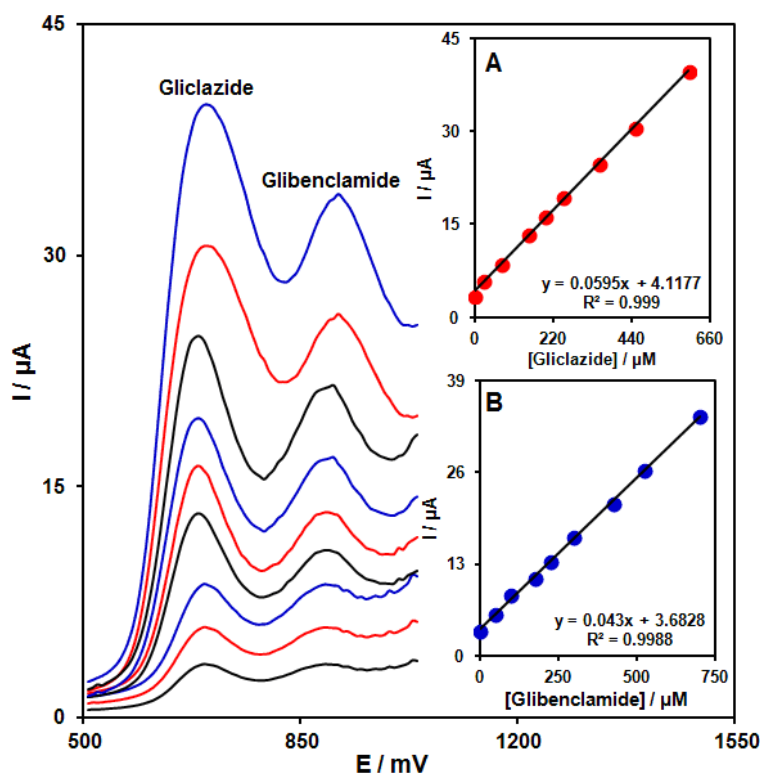


Figure 11. DPVs obtained at the surface of Fe_3O_4 NP/SPE for different concentrations of gliclazide and glibenclamide. DPVs from inner to outer correspond to 2.0+2.0, 25.0+50.0, 75.0+100.0, 150.0+175.0, 200.0+225.0, 250.0+300.0, 350.0+425.0, 450.0+525.0 and 600.0+700.0 μ M of gliclazide + glibenclamide, respectively. Insets: (A) plots of I_p vs. gliclazide concentration and (B) plot of I_p vs. glibenclamide concentration.

In order to make such a test, gliclazide and glibenclamide were concurrently analyzed using different concentrations of each in DPV experiments with the mentioned NP/SPEs as the working electrodes, and the results are given in Figure 11. Two well-defined anodic peaks for gliclazide and glibenclamide at 700 and 900 mV can clearly be distinguished in Figure 11, suggesting the applicability of the modified electrode to the concurrent determination of these two compounds.

3.6. Analysis of real samples

3.6.1. Pharmaceutical preparations

The samples were prepared as mentioned above and were next spiked with specified concentration of gliclazide and glibenclamide.

Table 2. Results of application of Fe₃O₄ NP/SPE for simultaneous determination of gliclazide and glibenclamide. All concentrations are in μM (n=5).

Sample	Spiked		Found		Recovery (%)		R.S.D. (%)	
	Gliclazide	Glibenclamide	Gliclazide	Glibenclamide	Gliclazide	Glibenclamide	Gliclazide	Glibenclamide
Gliclazide tablet	0	0	10.0	ND ^a	-	-	3.2	-
	2.5	5.0	12.2	5.1	97.6	102.0	1.9	3.3
	5.0	10.0	15.2	9.8	101.3	98.0	2.8	1.7
	7.5	15.0	18.1	14.9	103.4	99.3	2.1	2.4
Glibenclamide tablet	10.0	20.0	19.8	20.3	99.0	101.5	2.4	2.3
	0	0	ND	5.0	-	-	-	2.9
	5.0	2.5	4.9	7.6	98.0	101.3	2.4	2.1
	10.0	7.5	10.1	12.2	101.0	97.6	2.1	1.8
	15.0	12.5	14.9	17.8	99.3	101.7	3.3	2.2
	20.0	17.5	20.7	22.3	103.5	99.1	1.9	3.1

ND: Not detected

Table 3. Comparison of the total values of gliclazide and glibenclamide of some pharmaceutical preparations determined using Fe₃O₄ NP/SPE (n=5) and declared values on sample labels.

Samples	Declared value	Found value	RSD%
Gliclazide tablet (mg per tablet)	10.0	10.1	2.5
Glibenclamide tablet (mg per tablet)	5.0	4.9	2.4

Table 4. Results of application of Fe₃O₄ NP/SPE for simultaneous determination of gliclazide and glibenclamide in urine samples (n=5). All concentrations are in μM (n=5).

Sample	Spiked		Found		Recovery (%)		R.S.D. (%)	
	Gliclazide	Glibenclamide	Gliclazide	Glibenclamide	Gliclazide	Glibenclamide	Gliclazide	Glibenclamide
Urine 1	5.0	7.5	4.9	7.7	98.0	102.7	3.2	1.6
	10.0	12.5	10.3	12.4	103.0	99.2	1.7	3.3
	15.0	17.5	15.2	17.1	101.3	97.7	2.9	2.4
	20.0	22.5	19.8	22.9	99.0	101.8	2.4	2.8
Urine 2	5.0	5.0	4.9	5.1	98.0	102.0	1.9	2.4
	7.5	10.0	7.7	9.9	102.7	99.0	2.2	2.6
	10.0	15.0	9.7	15.5	97.0	103.3	3.1	1.7
	12.5	20.0	12.7	19.5	101.6	97.5	2.5	3.2

The tests were based on the repeated DPV (n=5) of the diluted analytes and the results are summarized in Table 1 together with relative standard deviations (RSD%) and recoveries of the spiked

samples that are all found at acceptable levels. The results were further compared with those declared on the labels of the pharmaceutical preparations (Table 3) and were found to be in good agreement. This would be the proof that the results obtained with the modified electrode, functionalized Fe₃O₄ NP/SPE, are dependable.

3.6.2. Urine samples

The method based on application of the modified electrode, the synthesized NP/SPE, was also applied to the determination of gliclazide and glibenclamide in urine samples. The results of determined gliclazide and glibenclamide contents in real samples shown in Table 3 indicate the satisfactory recovery of the analytes. The reproducibility of the results obtained using the method is established in terms of R.S.D.

4. CONCLUSION

The research was focused on the fabrication of gliclazide/glibenclamide sensor, which was performed through modifying a SPE with functionalized Fe₃O₄ NP (Fe₃O₄ NP/SPE). The results of CV and DPV analyses based on using this modified electrode have indicated that oxidation of gliclazide is optimal at pH=7.0. Also, when using this prepared Fe₃O₄ NP/SPE as the working electrode, the peak potential of gliclazide was found to move for about 140 mV towards less positive values. In detecting gliclazide and glibenclamide, the sensor was found to offer advantages of low detection limits of 1.0×10^{-7} M and 9.0×10^{-7} M and rather wide linear ranges of 5.0×10^{-7} – 6.0×10^{-4} M and 2.0×10^{-6} – 7.0×10^{-4} M for gliclazide and glibenclamide, respectively. This was attributed to the increased effective surface area of the electrode as a result of the modification which led to low detection limits. The modified electrode was also found to be successfully applicable for the concurrent determination of both analytes, what cannot be achieved using unmodified SPE. The results of the present work are expected to act as effective steps towards the fabrication of novel electrochemical sensors for determination of gliclazide and glibenclamide.

References

1. S. Ristic, C. Collober-Maugeais, E. Pecher, and F. Cressier, *Diabetic Med.*, 23 (2006) 757.
2. C. M. Sena, T. E. R. E. S. A. Louro, P. A. U. L. O. Matafome, E. L. S. A. Nunes, P. E. D. R. O. Monteiro, and R. A. Q. U. E. L. Seça, *Seça, Physiol. Res.*, 58 (2009) 203.
3. N. El-Enany, *Farmaco*, 59 (2004) 63.
4. M. R. Rouini, A. Mohajer, and M. H. Tahami, *J. chromatogr B*, 785 (2003) 383.
5. J. Krzek, M. Dabrowska, and U. Hubicka, *J. Planar Chromat.*, 14 (2001) 183.
6. J. Lv, Q. Wang, X. Chen, P. He, and Y. Fang, *J. Pharm. Biomed. Anal.*, 39 (2005) 843.
7. G. P. Zhong, H. C. Bi, S. Zhou, X. Chen, and M. Huang, *J. Mass Spectrum.*, 40 (2005) 1462.
8. Y. K. Agrawal, P. J. Gogoi, K. Manna, H. G. Bhatt, and V. K. Jain, *Indian j. pharm. sci.*, 72 (2010) 50.
9. H. Hrichi, M. R. Louhaichi, L. Monser, and N. Adhoum, *Sens. Actuators B Chem.*, 204 (2014) 42.
10. A. E. Radi, and S. Eissa, *Electroanalysis*, 22 (2010) 2991.

11. E. Pourtaheri, M. A. Taher, G. A. Ali, S. Agarwal, V. K. Gupta, *J. Mol. Liq.*, 289 (2019) 111141.
12. P. Cryer, *Diabetologia*, 45 (2002) 937.
13. N. L. Delgadillo-Armendariz, N. A. Rangel-Vázquez, and A. I. García-Castañón, *Spectrochim. Acta Mol. Biomol. Spectrosc.*, 120 (2014) 524.
14. C. J. Tack, and P. Smits, *Neth. J. med.* 55 (1999) 209.
15. S. J. Park, Y. J. Lee, D. N. Heo, I. K. Kwon, K. S. Yun, J. Y. Kang, and S. H. Lee, *Sens. Actuators B Chem.*, 215, (2015) 133.
16. S. Tajik, M. A. Taher, H. Beitollahi, and M. Torkzadeh-Mahani, *Talanta*, 134 (2015) 60.
17. H. Karimi-Maleh, and O. A. Arotiba, *J. Colloid Interf. Sci.*, 560 (2020) 208.
18. H. Beitollahi, H. Karimi-Maleh, and H. Khabazzadeh, *Anal. Chem.*, 80 (2008) 9848.
19. NA. Nowroozi, P. Mohammadzadeh Jahani, N. Asli, H. Hajiabadi, S. Dahmardeh, H. Raissi, *Int. J. Quant. Chem.*, 112 (2012) 489.
20. M. Mazloun-Ardakani, H. Beitollahi, M. K. Amini, F. Mirkhalaf, B. F. Mirjalili, and A. Akbari, *Analyst*, 136 (2011) 1965.
21. N. A. Nowroozi, H. Roohi, M. Poorsargol, P. Mohammadzadeh Jahani, H. Hajiabadi, H. Raissi, *Int. J. Quant. Chem.*, 111 (2011) 3008.
22. H. Beitollahi, M. Hamzavi, and M. Torkzadeh-Mahani, *Mater. Sci. Eng. C*, 52 (2015) 297.
23. N. Chauhan, S. Chawla, C. S. Pundir, and U. Jain, *Biosens. Bioelectron.*, 89 (2017) 377.
24. H. Beitollahi, S. Tajik, M. H. Asadi, and P. Biparva, *J. Anal.Sci. Technol.*, 5 (2014) 29.
25. Y. Yu, M. Guo, M. Yuan, W. Liu, and J. Hu, *Biosens. Bioelectron.*, 77 (2016) 215.
26. M. Kazemipour, M. Ansari, A. Mohammadi, H. Beitollahi, and R. Ahmadi, *J. Anal. Chem.*, 64 (2009) 65.
27. P. Mohammadzadeh Jahani, A. Nowroozi, H. Hajiabadi, M. Hassani, *Struct. Chem.*, 23 (2012) 1941.
28. A. Taherkhani, T. Jamali, H. Hadadzadeh, H. Karimi-Maleh, H. Beitollahi, M. Taghavi, and F. Karimi, *Ionics*, 20 (2014) 421.
29. H. Karimi-Maleh, C. T. Fakude, N. Mabuba, G. M. Peleyeju, and O. A. Arotiba, *J. colloid Interf. Sci.*, 554 (2019) 603.
30. H. Beitollahi, M. M. Ardakani, H. Naeimi, and B. Ganjipour, *J. Solid State Electrochem.*, 13 (2009) 353.
31. R. Shi, J. Liang, Z. Zhao, A. Liu, and Y. Tian, *Talanta*, 169 (2017) 37.
32. H. Soltani, H. Beitollahi, A. H. Hatefi-Mehrjardi, S. Tajik, and M. Torkzadeh-Mahani, *Anal. Bioanal. Electrochem.*, 6 (2014) 67.
33. Y. Li, X. Zhai, X. Liu, L. Wang, H. Liu, and H. Wang, *Talanta*, 148 (2016) 362.
34. S. Tajik, and H. Beitollahi, *Anal. Bioanal. Chem. Res.*, 6 (2019) 171.
35. V. Sethuraman, P. Muthuraja, J. A. Raj, and P. Manisankar, *Biosens. Bioelectron.*, 84 (2016) 112.
36. S. Esfandiari-Baghamidi, H. Beitollahi, S. Tajik, and R. Hosseinzadeh, *Int. J. Electrochem. Sci.*, 11 (2016) 10874.
37. H. Beitollahi, F. Ebadinejad, F. Shojaie, and M. Torkzadeh-Mahani, *Anal. Methods*, 8 (2016) 6185.
38. G. G. Gerent, and A. Spinelli, *J. Hazard. Mater.*, 330 (2017) 105.
39. H. Beitollahi, M. Mazloun-Ardakani, H. Naeimi, and B. Ganjipour, *J. Solid State Electrochem.*, 13 (2009) 353.
40. S. D. Bukkitgar, and N. P. Shetti, *Mater. Sci. Eng C*, 65 (2016) 262.
41. M.R. Ganjali, Z. Dourandish, H. Beitollahi, S. Tajik, L. Hajiaghababaei, and B. Larijani, *Int. J. Electrochem. Sci.*, 13 (2018) 2448.
42. P. S. Dorraji, and F. Jalali, *Food chem.*, 227 (2017) 73.
43. S. Tajik, M. A. Taher, and H. Beitollahi, *Ionics*, 20 (2014) 1155.
44. H. Mahmoudi-Moghaddam, S. Tajik, and H. Beitollahi, *Food chem.*, 286 (2019) 191.
45. S. Easwaramoorthi, and P. Natarajan, *Mater. Chem. Phys.*, 107 (2008) 101.
46. H. M. Moghaddam, H. Beitollahi, S. Tajik, M. Malakootian, and H. K. Maleh, *Environ. Monit.*

- Asses., 186 (2014) 7431.
47. H. Beitollahi, F. Movahedifar, S. Tajik, and Sh.Jahani, *Electroanalysis*, 31 (2019) 1195.
 48. S. Tajik, H.Beitollahi, and P.Biparva, *J. Serb. Chem. Soc.*, 83 (2018) 863.
 49. Z. Wei, Y. Yang, X. Xiao, W. Zhang, and J. Wang, *Sens. Actuators B Chem.*, 255 (2018) 895.
 50. H. Beitollahi, S. Tajik, S. Z. Mohammadi, and M. Baghayeri, *Ionics*, 20 (2014) 571.
 51. J.Agrisuelas, M. I. González-Sánchez, and E.Valero, *Sens. Actuators B Chem.*, 249 (2017) 499.
 52. H. Beitollahi, Z. Dourandish, S. Tajik, M. R. Ganjali, P. Norouzi, and F. Faridbod, *J. Rare Earth.*, 36 (2018) 750.
 53. M. Govindasamy, V.Mani, S. M. Chen, T. W. Chen, and A. K. Sundramoorthy, *Scien. Rep.*, 7 (2017) 46471.
 54. H. Beitollahi, S. Tajik, M.R. Aflatoonian, and A. Makarem, *Anal. Bioanal. Electrochem.*, 10 (2018) 1399.
 55. S. Rana, S. K. Mittal, N. Singh, J. Singh, and C. E. Banks, *Sens. Actuators B Chem.*, 239 (2017) 17.
 56. H. Beitollahi, H. Mahmoudi-Moghaddam, and S. Tajik, *Anal. Lett.*, 52 (2019) 1432.
 57. S. X. Lee, H. N. Lim, I. Ibrahim, A. Jamil, A. Pandikumar, and N. M. Huang, *Biosens. Bioelectron.*, 89 (2017) 673.
 58. F. Garkani-Nejad, H. Beitollahi, and R. Alizadeh, *Anal. Bioanal. Electrochem.*, 9(2017) 134.
 59. Y. M. Zhang, P. L. Xu, Q. Zeng, Y. M. Liu, X.Liao, M. F. Hou, *Mater. Sci. Eng C*, 74 (2017) 62.
 60. L. Ma, M. Liu, T. Peng, K. Fan, L. Lu, and K. Dai, *Mater. Chem. Phys.*, 118 (2009) 477.
 61. S. Tajik, F. Garkani-Nejad, and H. Beitollahi, *Russ. J. Electrochem.*, 55 (2019) 314.
 62. M. A. Khalilzadeh, S. Tajik, H. Beitollahi, and R. A. Venditti, *Ind. Eng. Chem. Res.*, 59 (2020) 4219.
 63. M. Safaei, H. Beitollahi, M.R. Shishehbore, S. Tajik, and R. Hosseinzadeh, *J. Serb. Chem. Soc.*, 84 (2019) 175.
 64. H. Beitollahi, F. Garkani-Nejad, S. Tajik, and M.R. Ganjali, *Iran. J. Pharm. Res.*, 18 (2019) 80.
 65. S. Z. Mohammadi, A. H. Sarhadi, and F. Mosazadeh, *Anal. Bioanal. Chem. Res.*, 5 (2018) 363.
 66. J. B. Raoof, R. Ojani, H. Beitollahi, and R. Hosseinzadeh, *Anal. Sci.*, 22 (2006) 1213.
 67. H. Mahmoudi-Moghaddam, H. Beitollahi, S. Tajik, I. Sheikshoaie, and P. Biparva, *Environ. Monit. Assess.*, 187 (2015) 407.
 68. Y. Wang, L. Wang, H. Chen, X. Hu, and S. Ma, *ACS Appl. Mater. Interfaces*, 8 (2016) 18173.
 69. H. Beitollahi, M. A. Khalilzadeh, S. Tajik, M. Safaei, K. Zhang, H.W. Jang, and M. Shokouhimehr, *ACS Omega*, 5 (2020) 2049.
 70. H. Beitollahi, R. Zaimbashi, M. Mahani, and S. Tajik, *Bioelectrochemistry*, 134 (2020) 107497.
 71. X. Fang, X. Chen, Y. Liu, Q. Li, Z. Zeng, T. Maiyalagan, and S. Mao, *ACS Appl. Nano Mater.*, 2 (2019) 2367.
 72. M. Mazloun-Ardakani, H. Beitollahi, M. K. Amini, B. F. Mirjalili, and F. Mirkhalaf, *J. Electroanal. Chem.*, 651(2011) 243.
 73. H. Beitollahi, M. Safaei, and S. Tajik, *Anal. Bioanal. Chem. Res.*, 6 (2019) 81.
 74. Q. Huang, X. Lin, L. Tong, and Q. X. Tong, *ACS Sustain. Chem. Eng.*, 8 (2020) 1644.
 75. M. M. Motaghi, H. Beitollahi, S. Tajik, and R. Hosseinzadeh, *Int. J. Electrochem. Sci.*, 11 (2016) 7849.
 76. S. Esfandiari-Baghamidi, H. Beitollahi, S. Z. Mohammadi, S. Tajik, S. Soltani-Nejad, and V. Soltani-Nejad, *Chin. J. Catal.*, 34 (2013) 1869.
 77. J. Chang, X. Wang, J. Wang, H. Li, and F. Li, *Anal. Chem.*, 91 (2019) 3604.
 78. M. Mazloun-Ardakani, H. Beitollahi, Z. Taleat, H. Naeimi, and N. Taghavinia, *J. Electroanal. Chem.*, 644 (2010) 1.
 79. S. Esfandiari-Baghamidi, H. Beitollahi, and S. Tajik, *Ionics*, 21(2015) 2363.
 80. M. Venu, S. Venkateswarlu, Y. V. M. Reddy, A. Seshadri Reddy, V. K. Gupta, M. Yoon, and G. Madhavi, *ACS Omega*, 3 (2018) 14597.

81. S. Tajik, M. A. Taher, H. Beitollahi, R. Hosseinzadeh, and M. Ranjbar, *Electroanalysis*, 28 (2016) 656.
82. H. Beitollahi, S. Tajik, H. Parvan, H. Soltani, A. Akbari, and M. H. Asadi, *Anal. Bioanal. Electrochem.*, 6 (2014) 54.
83. Y. Wang, L. Wang, H. Chen, X. Hu, and S. Ma, *ACS Appl. Mater. Interfaces*, 8 (2016) 18173.
84. H. Mahmoudi- Moghaddam, S. Tajik, and H. Beitollahi, *Microchem. J.*, 150 (2019) 104085.
85. M. R. Ganjali, H. Beitollahi, R. Zaimbashi, S. Tajik, M. Rezapour, and B. Larijani, *Int. J. Electrochem. Sci.*, 13 (2018) 2519.
86. J. Yang, P. Wang, X. Zhang, and K. Wu, *J. Agric. Food Chem.*, 57 (2009) 9403.
87. E. Manova, T. Tsoncheva, C. Estournès, D. Paneva, K. Tenchev, I. Mitov, and L. Petrov, *Appl. Catal A*, 300 (2006) 170.
88. C. Yu, L. Gou, X. Zhou, N. Bao, and H. Gu, *Electrochim. Acta*, 56 (2011) 9056.
89. S. Laurent, D. Forge, M. Port, A. Roch, C. Robic, L. Vander Elst, and R. N. Muller, *Chem. Rev.*, 108 (2008) 2064.
90. L. Shen, P. E. Laibinis, and T. A. Hatton, *Langmuir*, 15 (1999) 447.
91. M. R. Ganjali, H. Salimi, S. Tajik, H. Beitollahi, M. Rezapour, and B. Larijani, *Int. J. Electrochem. Sci.*, 12 (2017) 5243.
92. J. Cao, Y. Wang, J. Yu, J. Xia, C. Zhang, D. Yin, and U. O. Häfeli, *J. Magn. Magn. Mater.*, 277 (2004) 165.
93. A. Jordan, R. Scholz, P. Wust, H. Schirra, T. Schiestel, H. Schmidt, and R. Felix, *J. Magn. Magn. Mater.*, 194 (1999) 185.
94. Q. Li, Y. Xuan, and J. Wang, *Exp. Therm. Fluid Sci.*, 30 (2005) 109.
95. M. M. Lakouraj, and H. Tashakkorian, *Supramol. Chem.*, 25 (2013) 221.
96. M. M. Lakouraj, and H. Tashakkorian, *J. Macromol. Sci. Part A*, 50 (2013) 310.
97. M. S. Darwish, N. H. Nguyen, A. Ševcù, and I. Stibor, *J. Nanomater.*, (2015).
98. A. Hasanpour, M. Niyafar, H. Mohammadpour, and J. Amighian, *J. Phys. Chem. Solids*, 73 (2012) 1066.
99. R. Chantrell, J. Popplewell, and S. Charles, *IEEE Trans. Magn.*, 14 (1978) 975.
100. A. J. Bard, Faulkner, L.R.; *Electrochemical Methods Fundamentals and Applications*, second ed, (Wiley, New York) (2001).

© 2020 The Authors. Published by ESG (www.electrochemsci.org). This article is an open access article distributed under the terms and conditions of the Creative Commons Attribution license (<http://creativecommons.org/licenses/by/4.0/>).